Inspection of formula (5.129) shows that under the given model assumptions, the glycolytic flux is only dependent on the kinetic parameters of the enzymes HK and PFK and on the equilibrium constant of PGI. It does not depend on the kinetic properties of the PK and the fast equilibrium enzymes. Therefore, the summation theorem for the normalized flux control coefficients assumes the form

$$C^J_{HK} + C^J_{PFK} = 1. \tag{5.139}$$

Because the parameters k_{HK} and k_{PFK} enter the rate laws of HK and PFK, respectively, in a linear manner the coefficients C^J_{HK} and C^J_{PFK} may be calculated as follows:

$$C^J_{HK} = \frac{\partial \ln J}{\partial \ln k_{HK}}, \quad C^J_{PFK} = \frac{\partial \ln J}{\partial \ln k_{PFK}}. \tag{5.140}$$

By use of Eq. (5.129) one gets

$$C^J_{HK} = 1 - C^J_{PFK} = 1 - \frac{a/2}{(1/2 + \sqrt{1/4 + a})\sqrt{1/4 + a}} \tag{5.141a}$$

with

$$a = \frac{k_{HK}\, ATP}{k_{PFK}\, q_{PGI}\, K_{I,G6P}}. \tag{5.141b}$$

One may easily see that

$$C^J_{HK} \geq C^J_{PFK} \tag{5.142}$$

always; that is, flux control is exerted mainly by the hexokinase, the first enzyme of the glycolytic pathway. Using the parameter values listed in Table 5.1 one obtains $C^J_{HK} = 0.69$ and $C^J_{PFK} = 0.31$. The participation of phosphofructokinase in flux control results from the feedback inhibition of hexokinase by G6P. An inhibition of the PFK, for example, would lead to an increase of its substrate F6P as well as of G6P, which would diminish the glycolytic flux by inhibition of the hexokinase. Elimination of the feedback inhibition of G6P ($K_{I,G6P} \to \infty$) would result in $C^J_{PFK} \to 0$ [cf. Eq. (5.141)].

Despite the higher control coefficient of the HK, the enzyme PFK may play an important role in the regulation of glycolysis owing to the high elasticity coefficients of a great number of internal and external effectors for this enzyme (see Otto *et al.*, 1974, 1977).

5.4.4.3. *Interplay of ATP Production and ATP Consumption*

Selkov (1975a, 1975b) proposed a skeleton model of glycolysis which, in contrast to Model A presented in Section 5.4.4.2, focuses on the production and degradation of ATP. It is described by the reaction scheme 12,

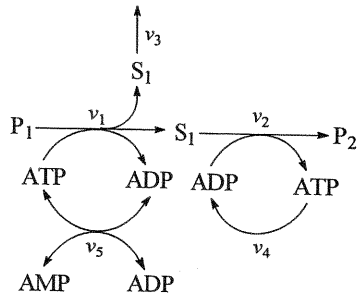

Scheme 12

where P_1 represents glucose and S_1 the pool of metabolites in the middle part of glycolysis. The ATP-consuming reactions of the upper part and the ATP-producing reactions of the lower part of glycolysis are lumped into reactions 1 and 2, respectively. v_3 represents the velocity of a side reaction without ATP production (describing, for example, the biosynthetic reactions leading to the synthesis of serine). v_4 denotes the rate of nonglycolytic ATP-consuming reactions (ATPases) and v_5 the rate of the adenylate kinase reaction (AK, EC 2.7.4.3). The model of Selkov has been modified by Heinrich and Rapoport (1975) by taking into account special features of erythrocyte glycolysis, in particular the 2,3P_2G bypass (Model B, see Figure 5.3). The reaction scheme results from that depicted in Figure 3.1

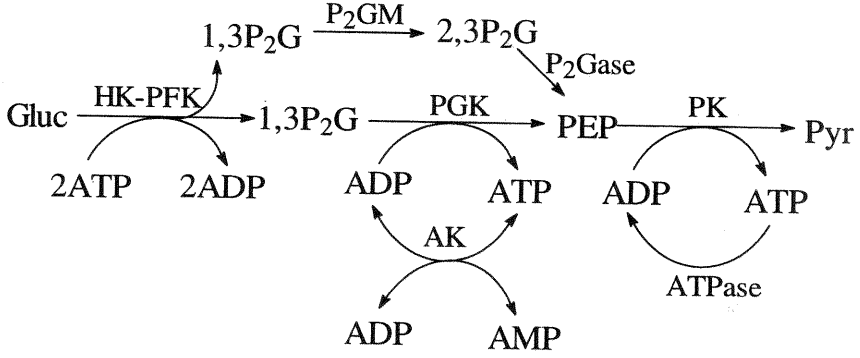

Figure 5.3 Simplified reaction scheme of erythrocyte glycolysis (Model B). The upper part of glycolysis (HK, PGI, PFK, Ald, TIM, GAPDH) are lumped into one reaction "HK-PFK." The lower part (PGAM, Enol, PK) is represented by the PK reaction

by some simplifications. Furthermore, the substrate inhibition of phosphofructokinase by ATP was included. Because the flux through the lower part of glycolysis is twice the flux through the upper part, 4 moles of ATP are produced at the reaction steps catalyzed by the enzymes PGK and PK, whereas 2 moles of ATP are consumed by the HK-PFK system. Accordingly, the degradation of 1 mole of glucose leads to the net production of 2 moles of ATP. The actual ATP production is decreased depending on the share of the $2,3P_2G$ bypass which circumvents the ATP-producing PGK reaction.

As in Model A, very simple rate laws were used for all enzymes. Except for the HK-PFK system, the activities of all enzymes were characterized by linear or bilinear relationships (see Table 5.2). Furthermore, all reactions are considered to be irreversible except for the adenylate kinase reaction (AK). For the sake of simplicity, the saturation of the P_2Gase by $2,3P_2G$ is neglected.

The factor $f(ATP)$ in the expression $v_{HK\text{-}PFK}$ (Table 3) describes the substrate inhibition of PFK by ATP. $K_{I,ATP}$ and n_H are the inhibition constant and the cooperativity coefficient, respectively, of the substrate inhibition by ATP.

Figure 5.4 shows the rate of the HK-PFK system as a function of ATP according to the rate law listed in Table 5.2. Two cases are considered: $n_H = 1$ (no substrate inhibition) and $n_H = 4$ (substrate inhibition). The kinetic constant $k_{HK\text{-}PFK}$ was adjusted in such a way that in both cases a rate $v_{HK\text{-}PFK} = 1.25$ mM/h was obtained for $ATP = 1.2$ mM (*in vivo* point P in Figure 5.4).

Using the rate law given in Table 5.2 one may calculate the elasticity coefficient for the HK-PFK system with respect to the ATP concentration. One obtains:

$$\varepsilon_{ATP}^{HK-PFK} = \frac{\partial \ln v_{HK-PFK}}{\partial \ln ATP} = \begin{cases} 0.45 & (n_H = 1) \\ -1.70 & (n_H = 4). \end{cases} \tag{5.143}$$

The dynamic properties of the model depicted in Figure 5.3 are governed by the following differential equations

$$\frac{d}{dt} 1,3P_2G = 2v_{HK-PFK} - v_{P_2GM} - v_{PGK}, \tag{5.144a}$$

$$\frac{d}{dt} 2,3P_2G = v_{P_2GM} - v_{P_2Gase}, \tag{5.144b}$$

$$\frac{d}{dt} PEP = v_{P_2Gase} + v_{PGK} - v_{PK}, \tag{5.144c}$$

$$\frac{d}{dt} AMP = -v_{AK}, \tag{5.144d}$$

$$\frac{d}{dt} ADP = 2v_{HK-PFK} - v_{PGK} - v_{PK} + v_{ATPase} + 2v_{AK}, \tag{5.144e}$$

Table 5.2 Rate Equations of Glycolytic Enzymes Included in Model B

$$v_{HK\text{-}PFK} = k_{HK\text{-}PFK} ATP \cdot f(ATP)$$

$$f(ATP) = \left[1 + \left(\frac{ATP}{K_{I,ATP}}\right)^{n_H}\right]^{-1}$$

$$v_{P_2GM} = k_{P_2GM} 1,3P_2G$$
$$v_{P_2Gase} = k_{P_2Gase} 2,3P_2G$$
$$v_{PGK} = k_{PGK} 1,3P_2G \cdot ADP$$
$$v_{PK} = k_{PK} PEP \cdot ADP$$
$$v_{AK} = k_{AK}^{+} AMP \cdot ATP - k_{AK}^{-} (ADP)^2$$
$$v_{ATPase} = k_{ATPase} ATP$$

$$\frac{d}{dt} ATP = -2v_{HK-PFK} + v_{PGK} + v_{PK} - v_{ATPase} - v_{AK}. \tag{5.144f}$$

From Eqs. (5.144d)–(5.144f), it follows that

$$\frac{d}{dt} (AMP + ADP + ATP) = 0, \tag{5.145a}$$

$$AMP + ADP + ATP = A = \text{const.}; \tag{5.145b}$$

that is, the sum A of the concentrations of the adenine nucleotides is a conserve quantity. Because adenylate kinase is a very fast enzyme, the rapid-equilibriur approximation can be applied to Eq. (5.144d). This leads to the following equi librium relation between the concentrations of the adenine nucleotides:

$$\frac{(ADP)^2}{AMP \cdot ATP} = q_{AK}. \tag{5.146}$$

Note that, when only steady states are considered, the adenylate kinase reactio could be considered to be at equilibrium even if it were not fast, because it rep resents a strictly detailed balanced reaction in the scheme given in Figure 5.3 (se Section 3.3.2). In system (5.144), the velocity v_{AK} may be eliminated by subtract ing Eq. (5.144d) from Eq. (5.144f),

$$\frac{d}{dt} (ATP - AMP) = -2v_{HK-PFK} + v_{PGK} + v_{PK} - v_{ATPase}, \tag{5.147}$$

following the procedure explained in Section 4.3. Equations (5.145b) and (5.146 represent two algebraic conditions for the concentrations of the adenine nuclec

Table 5.3 Values of Parameters and Steady-State Values of Variables of Erythrocyte Glycolysis (Model B)

Parameter	Value
$k_{HK\text{-}PFK}$	3.20/h
k_{P_2GM}	1500/h
k_{P_2Gase}	0.15/h
k_{PGK}	$1.57 \cdot 10^4$/mM h
k_{PK}	559/mM h
k_{ATPase}	1.46/h
n_H	4.0
$K_{I,ATP}$	1.0 mM
q_{AK}	2.0
A	1.5 mM
Variable	**Value**
Metabolite Concentrations (mM)	
$1,3P_2G$	0.0005
$2,3P_2G$	5.0
PEP	0.02
AMP	0.076
ADP	0.22
ATP	1.20
Metabolic Fluxes (mM/h)	
$v_{HK\text{-}PFK}$ $(=J)$	1.25
v_{P_2GM}	0.75
v_{P_2Gase}	0.75
v_{PGK}	1.75
v_{PK}	2.50
v_{ATPase}	1.75

tides. Accordingly, the concentrations of AMP and ADP may be expressed by the concentration of ATP:

$$ADP = A\left[-\frac{q_{AK}}{2} + \sqrt{\frac{q_{AK}^2}{4} + q_{AK}\frac{ATP}{A}\left(1 - \frac{ATP}{A}\right)}\right] = g_1(ATP), \quad (5.148a)$$

$$AMP = A - g_1(ATP) - ATP = g_2(ATP). \quad (5.148b)$$

The functions $ADP = g_1(ATP)$ and $AMP = g_2(ATP)$ are represented graphically in Figure 5.5.

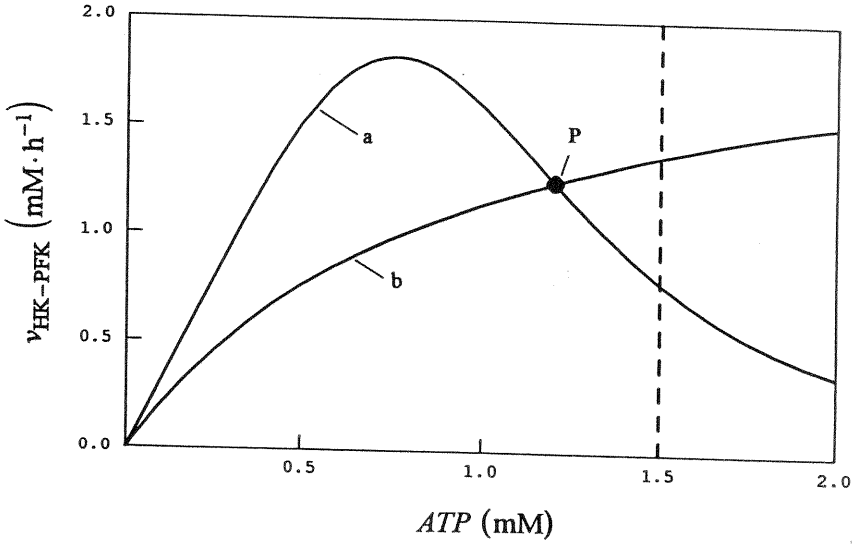

Figure 5.4 Glycolytic rate $v_{HK\text{-}PFK}$ as a function of the ATP concentration according to the rate law of the HK-PFK system given in Table 5.2. Parameter values: curve a, $n_H = 4$, $k_{HK\text{-}PFK} = 3.20$ h^{-1}; curve b, $n_H = 1$, $k_{HK\text{-}PFK} = 2.29$/h; P: *in vivo* point; broken line: $ATP = A$.

It is seen that the concentration of AMP decreases monotonically with increasing ATP concentration, whereas the function for ADP displays a maximum and becomes zero for $ATP = 0$ and $ATP = A$.

The left-hand side of Eq. (5.147) may be rewritten as follows

$$\frac{d}{dt}(ATP - AMP) = \left(1 - \frac{dAMP}{dATP}\right)\frac{dATP}{dt}. \quad (5.149)$$

From Eqs. (5.147) and (5.149), it follows that

$$\frac{d}{dt}ATP = \left(1 - \frac{dAMP}{dATP}\right)^{-1}(-2v_{HK-PFK} + v_{PGK} + v_{PK} - v_{ATPase}). \quad (5.150)$$

The differential equation system (5.144) can now be reduced in dimension by replacement of Eqs. (5.144d)–(5.144f) by the algebraic conditions (5.148a) and (5.148b) and the differential equation (5.150).

Stationary states are defined by vanishing time derivatives of the metabolite concentrations. One obtains from Eqs. (5.144a)–(5.144c) and (5.150)

$$2v_{HK-PFK} - v_{P_2GM} - v_{PGK} = 0, \quad (5.151a)$$

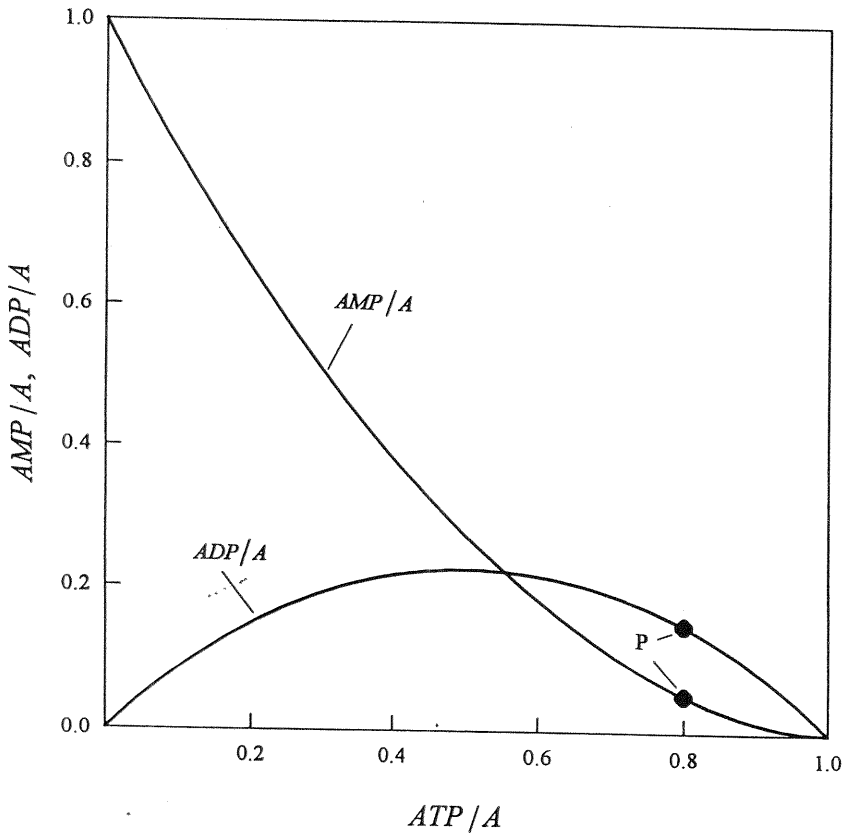

Figure 5.5 Interrelation between the concentrations of adenine nucleotides according to Eqs. (5.148a) and (5.148b) for $q_{AK} = 2$; P: *in vivo* point.

$$v_{P_2GM} - v_{P_2Gase} = 0, \tag{5.151b}$$

$$v_{P_2Gase} + v_{PGK} - v_{PK} = 0, \tag{5.151c}$$

$$-2v_{HK-PFK} + v_{PGK} + v_{PK} - v_{ATPase} = 0. \tag{5.151d}$$

Summation of Eqs. (5.151a)–(5.151d) yields

$$v_{PGK} = v_{ATPase} \tag{5.152}$$

and, by use of the kinetic equations listed in Table 5.2,

$$k_{PGK}ADP \cdot 1{,}3P_2G = k_{ATPase}ATP. \tag{5.153}$$

Because under steady-state conditions the ATP production in the PK step is compensated by the ATP consumption by the HK-PFK system ($2v_{HK\text{-}PFK} = v_{PK}$), Eqs. (5.152) and (5.153) characterize the balance between ATP-consuming and ATP-producing processes. For the calculation of the ATP concentration by use of Eq. (5.153), the concentration of $1{,}3P_2G$ is eliminated by consideration of Eq. (5.151a), which reads, in more detail,

$$2k_{HK-PFK}ATP \cdot f(ATP) - k_{P_2GM} \cdot 1{,}3P_2G - k_{PGK} \cdot 1{,}3P_2G \cdot ADP = 0. \tag{5.154}$$

This entails

$$1{,}3P_2G = \frac{2k_{HK-PFK}ATP \cdot f(ATP)}{k_{P_2GM} + k_{PGK}ADP}. \tag{5.155}$$

Inserting Eq. (5.155) into Eq. (5.153) yields

$$v_{PGK} = \frac{2k_{HK-PFK}k_{PGK}ADP \cdot ATP \cdot f(ATP)}{k_{P_2GM} + k_{PGK}ADP} = k_{ATPase}ATP = v_{ATPase}, \tag{5.156}$$

where the concentration of ADP must be considered as a function of ATP [cf. Eq. (5.148a)].

Figure 5.6 shows the net rate of the glycolytic ATP production (v_{PGK}) and the rate of the nonglycolytic ATP consumption (v_{ATPase}) as functions of the ATP concentration for various values of the rate constant of the ATPase. The values of the kinetic parameters (see Table 5.3) are close to those found in human erythrocytes. The intersection points of the curves $v_{PGK}(ATP)$ and $v_{ATPase}(ATP)$ determine the steady-state values of the ATP concentration. Evidently, the point $ATP = 0$ represents a trivial steady state which is a solution of Eq. (5.156) irrespective of the values of the kinetic parameters (state P_0). It is further seen that above a critical value, k^{crit}_{ATPase} (curve a), only the trivial steady state is obtained. For $k_{ATPase} < k^{crit}_{ATPase}$, two steady states P_1 and P_2 are found, in addition to the trivial steady state. A detailed stability analysis which is based on a linearization of the equation system (5.144a)–(5.144c), (5.145), (5.148) and (5.150) and computation of the eigenvalues of the corresponding Jacobian (see Section 2.3.2), reveals that the states with low (nonvanishing) ATP concentration (states P_1) are unstable, whereas the steady states with high ATP concentration (states P_2) are stable. One may conclude that the steady state found *in vivo* corresponds to the stable high-energy state P_2.

The curves depicted in Figure 5.7 show the steady state concentration of ATP as a function of k_{ATPase} for $n_H = 1$ and $n_H = 4$. Stable and unstable states are

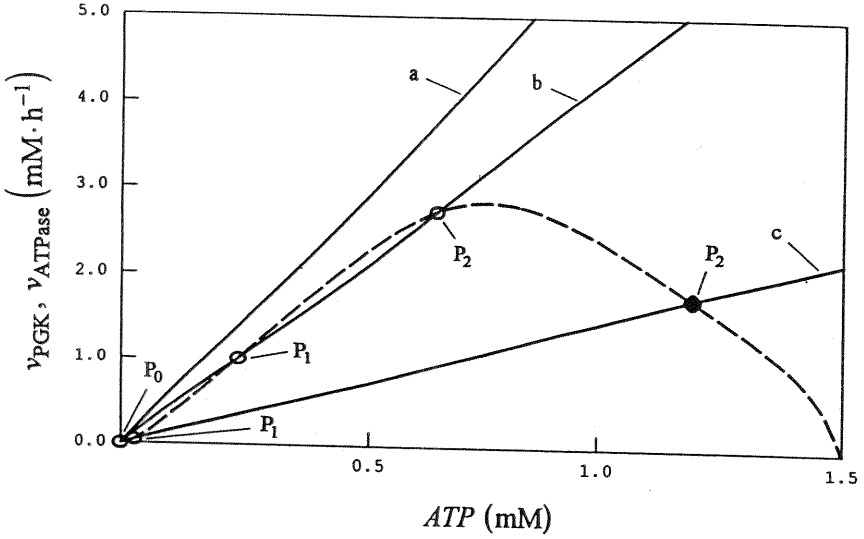

Figure 5.6 Rates of the enzymes ATPase (solid lines) and PGK (broken line) as functions of the ATP concentration according to Eq. (5.156). The intersection points P_0, P_1, and P_2 correspond to steady states. The intersection point P_2 on curve c is the *in vivo* point. Parameter values: curve a, k_{ATPase} = 5.83/h; curve b, k_{ATPase} = 4.23/h; curve c, k_{ATPase} = 1.46/h. The values of the other parameters correspond to those listed in Table 5.3.

characterized by solid and broken lines, respectively. It becomes clear that the critical values k_{ATPase}^{crit} represent bifurcation points which separate parameter regions with different numbers of steady states.

Figure 5.8 shows the steady-state concentration of ATP as a function of the rate of the ATPase for various values of the cooperativity coefficient (n_H) of the ATP-substrate inhibition of the HK-PFK system. The curves for high n_H values are characterized by the property that in the neighborhood of the *in vivo* state, the ATP concentration is rather insensitive against variations of the ATP-consumption rate. The regulatory property of glycolysis which leads to homeostasis of the ATP concentration in face of variations of the rate of ATP consumption was extensively studied by Selkov (1975b).

There are two reasons for ATP homeostasis. First, the share of the $2,3P_2G$ bypass $v_{P_2GM}/2v_{HK\text{-}PFK}$ decreases with increasing ATP-consumption rate. According to the steady-state equation (5.151a)

$$\frac{v_{PGK}}{2v_{HK-PFK}} = 1 - \frac{v_{P_2GM}}{2v_{HK-PFK}}, \qquad (5.157)$$

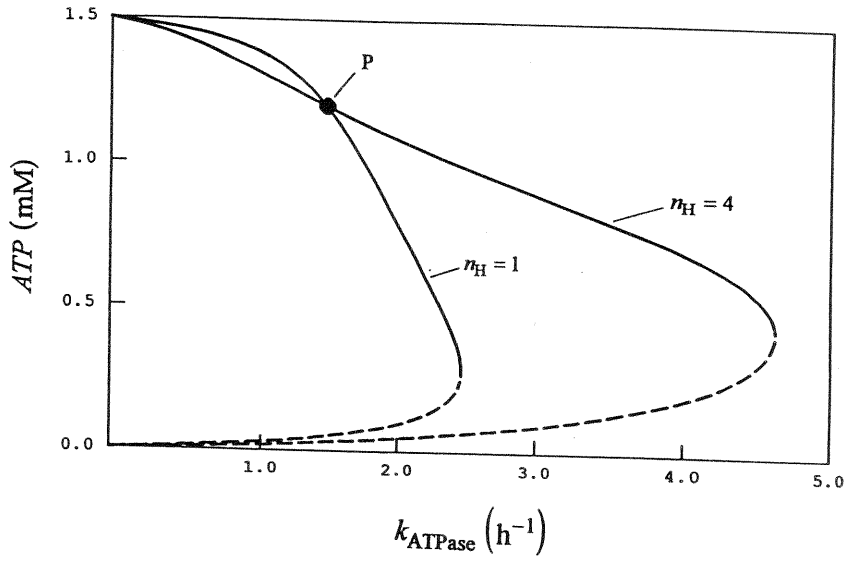

Figure 5.7 ATP concentration as a function of the rate constant k_{ATPase} for two different values of the cooperativity coefficient of the ATP inhibition of PFK (n_H = 1 and n_H = 4). Solid and broken lines indicate stable and unstable steady states, respectively.

a decrease of $v_{P_2GM}/2v_{HK\text{-}PFK}$ is accompanied by an increase of the share of the ATP-producing PGK reaction which meets the higher demand on ATP. A second effect contributing even more to homeostasis is the activation of the glycolytic flux at decreasing ATP concentration, which results from a lowering of the ATP inhibition (Figure 5.9).

In Table 5.4 the control coefficients are listed for the glycolytic flux ($J = v_{HK\text{-}PFK}$) and for the concentrations of the metabolites ATP and $2,3P_2G$. It is seen that in contrast to Model A, not only the HK and PFK but also the enzymes P_2GM, P_2Gase and ATPase exhibit nonvanishing flux control coefficients. This result is due to the circumstance that the upper and lower parts of the glycolytic system are coupled by the common cofactors ATP and ADP. Nevertheless the HK-PFK system is mainly responsible for flux control, such as in Model A. The calculations were performed for the *in vivo* state under the assumption $n_H = 1$ (no substrate inhibition of HK-PFK by ATP) and $n_H = 4$ (substrate inhibition of HK-PFK by ATP). It is seen that for $n_H = 1$, the flux control coefficient of ATPase is negative because the decrease of ATP after activation of ATPase leads to a diminution of the rate $v_{HK\text{-}PFK}$. In the more realistic case ($n_H = 4$), a decrease of ATP will activate glycolysis so that the flux control coefficient of ATPase becomes positive. The control coefficients for ATP may be considered as a quantitative

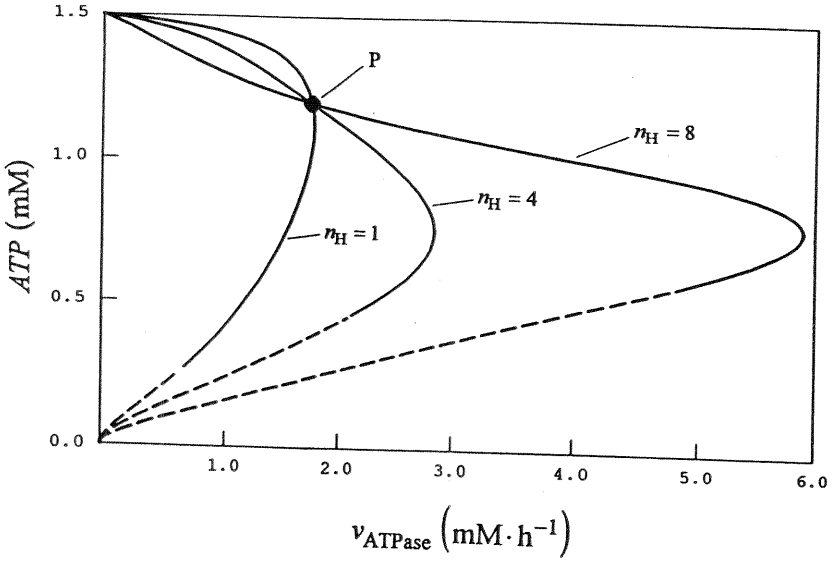

Figure 5.8 ATP concentration as a function of the rate $v_{ATPase} = k_{ATPase} ATP$ of ATP-consuming processes for different values of n_H and $k_{HK\text{-}PFK}$. Parameter values: $k_{HK\text{-}PFK} = 2.29/h$ ($n_H = 1$); $k_{HK\text{-}PFK} = 3.20/h$ ($n_H = 4$); $k_{HK\text{-}PFK} = 5.52/h$ ($n_H = 8$). Broken lines indicate unstable steady states. P: *in vivo* point.

measure for the ATP homeostasis, as already discussed. The homeostatic effect of the substrate inhibition is expressed by the fact that for $n_H = 4$ the coefficients $C^{ATP}_{HK\text{-}PFK}$ and C^{ATP}_{ATPase} are small compared to those obtained for $n_H = 1$. It is seen that the substrate inhibition of HK-PFK by ATP results not only in a homeostasis of *ATP* but also of $2,3P_2G$.

The flux control coefficients of the enzymes P_2GM and PGK are of opposite sign. The negative value of C^J_{PGK} for $n_H = 4$ is easily understood by consideration of the fact that activation of PGK results in diminution of the $2,3P_2G$ bypass and, in this way, to an increase in ATP concentration.

Under the assumptions of this model, the pyruvate kinase reaction neither controls the concentrations of ATP and $2,3P_2G$ nor the glycolytic flux. This results from the simplifying assumption that the PGK reaction is irreversible. The control coefficients for the glycolytic flux and for the metabolite concentrations listed in Table 5.4 sum up to unity and zero, respectively, that is, they fulfill the summation theorems.

An extension of Model B of glycolysis was set up to study the influence of pyruvate kinase deficiency on the energy metabolism of human erythrocytes (Holzhütter *et al.*, 1985b). A new comprehensive kinetic model of the pyruvate kinase of human erythrocytes was included and account was taken of the magnesium-

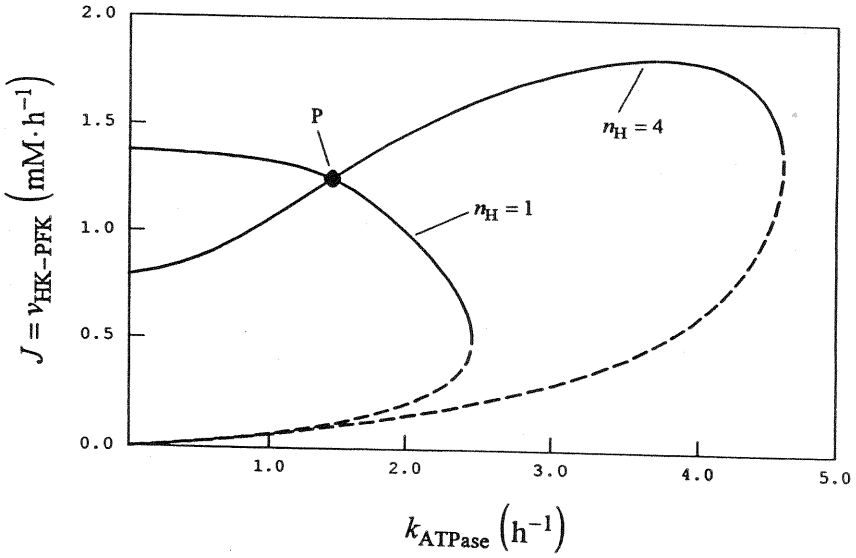

Figure 5.9 Glycolytic rate $J = v_{HK\text{-}PFK}$ as a function of the rate constant k_{ATPase} for two different values of n_H. Parameter values: $k_{HK\text{-}PFK} = 2.29\ h^{-1}$ ($n_H = 1$); $k_{HK\text{-}PFK} = 3.20\ h^{-1}$ ($n_H = 4$). P: *in vivo* point.

Table 5.4 Control Coefficients of Enzymes for the Glycolytic Flux and Metabolite Concentrations (Model B)

	Variable					
	$v_{HK\text{-}PFK}(=J)$		*ATP*		$2,3P_2G$	
Enzyme	$n_H = 1$	$n_H = 4$	$n_H = 1$	$n_H = 4$	$n_H = 1$	$n_H = 4$
HK-PFK	1.32	0.52	0.72	0.28	2.74	1.07
P_2GM	−0.10	0.14	−0.22	−0.08	0.18	0.68
P_2Gase	0.00	0.00	0.00	0.00	−1.00	−1.00
PGK	0.10	−0.14	0.22	0.08	−0.18	−0.68
ATPase	−0.32	0.48	−0.72	−0.28	−1.74	−0.07
$\sum_j C_j$	1.00	1.00	0.00	0.00	0.00	0.00

complex formation of the adenine nucleotides and 2,3-biphosphoglycerate. The analysis of individual cases with pyruvate kinase mutations permitted estimates and classification of the degree of disorder of the glycolytic pathway, which were in accord with clinical and other experimental assessments.

Other extensions consider the coupling of the glycolytic pathway with reactions responsible for the synthesis and breakdown of adenine nucleotides, in particular the 5′-nucleotidase (EC 3.1.3.5), AMP deaminase (EC 3.5.4.6), adenosine kinase (EC 2.7.1.20), adenine phosphoribosyltransferase (EC 2.4.2.7) and the uptake of adenosine across the erythrocyte membrane (Schauer *et al.* 1981a, 1981b). The main effect of including these reactions is that the total sum of the adenine nucleotides is no longer a conserved quantity. This model allows one to simulate the breakdown of adenine nucleotides after glucose depletion.

R. Schuster *et al.* (1988) developed a model of erythrocyte metabolism which comprises, in addition to glycolysis, the pentose phosphate pathway. Special attention is drawn to the fact that in erythrocytes the main function of the pentose phosphate shunt is to form NADPH. The NADPH produced by the two dehydrogenases (glucose-6-phosphate dehydrogenase, G6PD, EC 1.1.1.49, and 6-phosphogluconate dehydrogenase, 6PGD, 1.1.1.43) is mainly utilized by the glutathione reductase (EC 1.6.4.2) catalyzing the reaction: GSSG + NADPH → 2GSH + NADP. Furthermore, an NADPH-dependent lactate dehydrogenase (I. Rapoport *et al.*, 1979) was included into the model. Steady states are calculated as functions of the rate constants k_{ATPase} and k_{Ox} representing the energetic load and the oxidative load, respectively, of the system. The calculation of flux control coefficients of the nonequilibrium reactions reveals that most of these coefficients are very small with the following main exceptions:

- **(a)** Nonglycolytic ATP-consuming processes (ATPases) which affect strongly the glycolytic rate, $C^{J}_{\mathrm{ATPase}} = 0.70$; see Model B for $n_{\mathrm{H}} = 4$ (Table 5.4).
- **(b)** 2,3-Bisphosphoglycerate phosphatase (P_2Gase) which controls the glycolytic flux and the reactions of the 2,3P_2G bypass, $C^{J}_{\mathrm{P_2Gase}} = 0.22$, $C^{J_{\mathrm{P_2GM}}}_{\mathrm{P_2Gase}} = 0.94$.
- **(c)** The reactions of the oxidative load affecting the reactions of the oxidative part of the pentose phosphate pathway, $C^{J_{\mathrm{G6PD}}}_{\mathrm{Ox}} = C^{J_{\mathrm{6PGD}}}_{\mathrm{Ox}} = 0.47$. It has been concluded that in the *in vivo* state of erythrocyte glycolysis, the 2,3P_2G bypass and the pentose phosphate pathway are almost independently controlled by the reactions consuming those metabolites which are produced by the corresponding pathways. The model was used for predicting the effect of glucose-6-phosphate dehydrogenase deficiencies (R. Schuster *et al.*, 1989) and was recently extended to predict the metabolic effect of large-scale enzyme activity alterations (R. Schuster and Holzhütter, 1995).

5.4.4.4. *Glycolytic Energy Metabolism and Osmotic States*

The theoretical investigation of energy metabolism in erythrocytes has been extended by inclusion of its interaction with active and passive fluxes of ions

across the cell membrane (Brumen and Heinrich, 1984; Werner and Heinrich, 1985). This model (Model C) allows one to evaluate the state of metabolism as well as osmotic and electric effects. Accordingly, control coefficients related to the volume can be calculated. (For a general treatment of the control of variables other than concentrations and fluxes, see Section 5.8.) Compared with previous models (e.g., Model B), the set of system parameters is enlarged by the quantities characterizing the electric charges and osmotic effects of hemoglobin, the permeabilities of ions, and the cell surface area.

The metabolic part of the "metabolic-osmotic model" is essentially based on the reduced reaction scheme used for Model B (Figure 5.3). Several assumptions and simplifications are used in the model:

- **(a)** The *in vivo* state is characterized by a fixed composition of the external medium.
- **(b)** The inhibitory actions of H^+ ions on the enzymes PFK and P_2GM are taken into account.
- **(c)** Two nonglycolytic ATP-consuming processes are considered: the Na/K-ATPase (EC 3.6.1.37) and the non-ion transport ATPases. It has been proposed that 25–70% of the ATP produced by glycolysis is utilized by the Na/K pump (Grimes, 1980). Maretzki *et al.* (1980) and Reimann *et al.* (1981) determined a value of 30%. The non-ion transport ATPases are linked to membrane phosphorylation processes.
- **(d)** Consideration of the transmembrane potential ($\Delta\Psi$) and of the cell water volume (V) as system variables necessitates the incorporation of detailed electric and osmotic conditions. It is assumed that the intracellular and extracellular compartments are electrically neutral and in osmotic equilibrium.

The differential equations for the concentrations of the glycolytic metabolites are easily derived from the reaction scheme (Figure 5.3). As the metabolite concentrations may also be changed by variations of the cell volume (V), one arrives at the following type of equation:

$$\frac{1}{V^0}\frac{\mathrm{d}(S_i V)}{\mathrm{d}t} = \sum_j n_{ij} v_j, \tag{5.158}$$

where S_i denotes the concentrations of 1,3P_2G, 2,3P_2G, PEP, and ATP [cf. Eqs. (5.144a)–(5.144c) and (5.150)]. V^0 represents the cellular volume in a reference state. For the enzymatic activities v_k rate laws are used which approximate the kinetic properties of the isolated enzymes. They are essentially the same as used in Model B. An exception is the rate equation for the Na/K-ATPase,

$$v_{\mathrm{Na/K-ATPase}} = \frac{k_{\mathrm{Na/K-ATPase}} \cdot ATP \cdot Na^+_{\mathrm{in}}}{1 + ATP/K_{\mathrm{m,ATP}}}, \tag{5.159}$$